Overview of TJ-II experiments

C. Alejaldre 1), J. Alonso 1), L. Almoguera 1), F. de Aragón 1), E. Ascasíbar 1), A. Baciero 1), R. Balbín 1), E. Blanco 1), J. Botija 1), B. Brañas 1), E. Calderón 1), A. Cappa 1), R. Carrasco 1), F. Castejón 1), J. R. Cepero 1), A.A. Chmyga 2), J. Doncel 1), N.B Dreval 2), S. Eguilior 1), L. Eliseev 3), T. Estrada 1), O. Fedyanin 4) , A. Fernández 1), J.M. Fontdecaba 5) , C. Fuentes 1), A. García 1), I. García-Cortés 1), B.Gonçalves 6) , J. Guasp 1), J. Herranz 1), A. Hidalgo 1), C. Hidalgo 1), J. A. Jiménez 1), I. Kirpitchev 1), S.M. Khrebtov 2), A.D. Komarov 2), A.S. Kozachok 2), L. Krupnik 2), F. Lapayese 1), M. Liniers 1), D. López-Bruna 1), A. López-Fraguas 1), J. López-Rázola 1) A López-Sánchez 1), E. de la Luna 1), R. Martín 1), M. Medrano 1), A.V.Melnikov 2), P. Méndez 1), K.J. McCarthy 1), F. Medina 1), B. van Milligen 1), I. S. Nedzelskiy 6), M. Ochando 1), J.L. de Pablos 1), L. Pacios 1), I. Pastor 1), M.A. Pedrosa 1), A. de la Peña 1), A. Petrov 4), S. Petrov 7), A. Portas 1), D. Rapisarda 1), J. Romero 1), L. Rodríguez-Rodrigo 1), E. Rodríguez-Solano 1), A. Salas 1), E. Sánchez 1), J. Sánchez 1), K. Sarksian 4), C. Silva 6), S. Schchepetov 4), N. Skvortsova 4), F. Tabarés 1), D. Tafalla 1), V. Tribaldos 1), J. Vega 1) and B. Zurro 1)

1) Laboratorio Nacional de Fusión. EURATOM-CIEMAT, 28040 Madrid, Spain
2) Institute of Plasma Physics, NSC KIPT, 310108 Kharkov, Ukraine
3) Institute of Nuclear Fusion, RNC Kurchatov Institute, Moscow, Russia
4) General Physics Institute, Russian Academy of Sciences, Moscow, Russia
5) Universitat Politècnica de Catalunya, Barcelona, Spain
6) Associação EURATOM/IST, Centro de Fusão Nuclear, 1049-001 Lisboa, Portugal
7) A.F. Ioffe Physical Technical Institute, 194021, St. Peterburg, Russia
e-mail contact of main author: carlos.hidalgo@ciemat.es

Abstract. This paper presents an overview of experimental results and progress made in investigating the role of magnetic configuration on stability and transport in the TJ-II stellarator. Global confinement studies have revealed a positive dependence of energy confinement on the rotational transform and plasma density, together with different parametric dependences for metallic and boronised wall conditions. Spontaneous and biasing-induced improved confinement transitions, with some characteristics that resemble those of previously reported H-mode regimes in other stellarator devices, have been observed. Also, magnetic configuration scan experiments have shown an interplay between magnetic structure (rationals, magnetic shear), transport and electric fields. Although the DC radial electric fields are comparable with those expected from neoclassical calculations, additional mechanisms based on neoclassical/turbulent bifurcations and kinetic effects are needed to explain the impact of magnetic topology on flows and radial electric fields. Local transport studies have demonstrated a dependence of plasma diffusivities and convective velocities on plasma density and heating power in consistency with global confinement properties. Hydrocarbon fuelling experiments in configurations with a low order rational value in the rotational transform located in the proximity of the last close flux surface ($n = 4/m = 2$) have shown the impurity screening properties related to the expected divertor effect. First experiments in NBI plasmas are reported.

1. Introduction

The TJ-II heliac ($B(0) \leq 1.2$ T, $R(0) = 1.5$ m, $\langle a \rangle \leq 0.22$ m $P_{ECH} \leq 600$kW, $P_{NBI} \leq 2$MW) offers unique peculiarities that make it a very suitable tool to investigate the complex phenomenology that interrelates electric field, instabilities, magnetic configuration and transport in fusion plasmas. It possesses a large range of achievable magnetic configurations ($0.9 \leq \iota(0)/2\pi \leq 2.2$) and low magnetic shear that allow for accurate control of the low-order rationals present in the rotational transform profile. Its magnetic well is the main stabilising

mechanism [1]. The magnetic well depth (up to 6%) can be almost suppressed in the edge region thereby making the rotational transform profile essentially constant.

The results presented in this paper have been obtained in plasmas created and heated with electron cyclotron resonance heating (ECRH) (2 x 300 kW gyrotrons, at 53.2 GHz, 2nd harmonic, X-mode polarisation) and Neutral Beam Injection (NBI) . The ECRH is coupled to the plasma through two quasi-optical transmission lines, placed at positions symmetric about the stellarator, and equipped with an internal steerable mirror. In this context, second harmonic breakdown simulations that take electron-electron collision processes into account have been performed [2] to compute the temporal evolution of different species and the breakdown time. First experiments with Neutral Beam Injection (NBI) heated plasmas have been performed in the TJ-II stellarator [3]. Beams of 400 kW port-through (H_0) power at 28 kV, are injected on to target plasmas created using one or two ECRH lines (200–400 kW). Ongoing developments include plasma heating by Bernstein waves (a new system is being design for TJ-II). In particular, the O-X-B1 scheme can provide full power deposition for densities above 1.3 x 10^{13} cm^{-3}.

The paper is organised as follows: In section 2, TJ-II global confinement and improved confinement regimes are reviewed. In section 3, recent transport studies are reported. Plasma wall studies are discussed in section 4. First properties of NBI plasmas are reported in section 5. Finally conclusions are presented in section 6.

2. Global confinement, enhanced confinement modes and magnetic topology

TJ-II global energy confinement time and plasma parameter dependencies have been investigated in metal and boronized wall conditions (Fig. 1). Previous experiments in all-metal wall conditions showed positive ι-dependence (0.5) and were roughly consistent with ISS95 predictions. A set of recent plasma discharges, produced in boronised wall conditions, exhibits better global confinement but yields different dependences on rotational transform (0.35) and, above all, on plasma density (1.06). The rotational transform-dependence of the boronised data set might still be considered marginally compatible with the ISS95 prediction but this is not the case with the density dependence. Possible physical origins for the differences observed between the all-metal and boronized data sets might include the impact on TJ-II global confinement of improved confinement regimes and/or plasma-wall interactions.

Spontaneous transitions and development of ExB sheared flows.

Spontaneous transitions to improved confinement regimes have already been observed in TJ-II. An enhanced particle confinement regime was found for plasmas created in an all-metal scenario [4]. It consists of a spontaneous transition to a highly peaked density profile mode that in turn leads to a decay in the electron density in the edge region and to an increase in total particle content. This mode leads to an increase in the global particle confinement time by a factor greater than three. The conditions under which the transition to this mode was achieved for all-metal walls included a predefined trimming of the gas-puff waveform and a critical density, $\langle n_e \rangle_{crit}$ ~6 x 10^{18} m^{-3}. For boronized-wall conditions the transition was obtained under different recycling/gas puffing conditions. Another type of spontaneous improvement in particle and energy confinement has been observed in some TJ-II plasmas. Again this is triggered by the only external knob [5], *i.e.* the fuelling rate.

Recent experiments have shown that the development of the naturally occurring edge velocity shear layer requires a minimum plasma density in the TJ-II stellarator (Fig. 1). The increasing in the edge shearing rate is correlated with the increase in turbulent velocity

fluctuations. These results, consistent with transition models of turbulence driven flows, might provide the underlying physics of spontaneous TJ-II transitions [6].

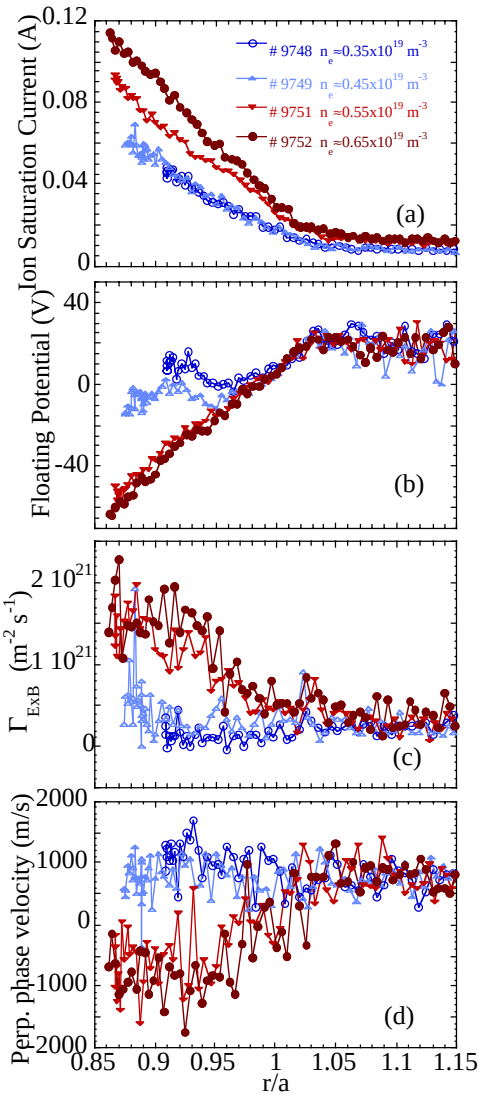

Figure 1. Radial profiles of (a) the ion saturation current, (b) the floating potential, (c) the local turbulent transport and (d) the deduced perpendicular velocity obtained for different values of the line averaged density in a plasma configuration with $\iota(a)/2\pi \approx 1.7$.

As plasma density increases, edge ion saturation current and its radial gradient increases, and the floating potential becomes more negative in the plasma edge. Because the edge temperature profile (in the range of 20 – 30 eV) is rather flat in the TJ-II plasma periphery, the radial variation in the floating potential signals directly reflects changes in the radial electric field (E_r), which turns out to be radially inwards in the plasma edge as density increases above 0.5 x 10^{19} m^{-3}. Local turbulent particle flux also shows an increase near the critical density and tends to slightly decrease as sheared flow develops. The magnitude of the spontaneous developed shearing rates have been compared with those measured during biasing induced improved confinement regimes in TJ-II (see below), suggesting that spontaneous sheared flows and fluctuations are near marginal stability. Electron density and temperature profiles evolution show a broadening in the density profile above the critical density while the temperature profile remains similar, reflecting the strong impact of plasma density in the TJ-II global confinement scaling.

Effect of transformer induced toroidal current in confinement.

Stellarators are currentless devices in which the only toroidal current sources are bootstrap and RF induced currents. In TJ-II, these currents can be compensated to some extent by means of the internal movable mirrors on the two quasi-optical ECRH lines. Also, the TJ-II has an ohmic (OH) transformer capable of inducing toroidal plasma currents up to 10 kA. Previously, it was found that plasma confinement improves by inducing a negative (with respect to the magnetic field) OH current [7]. Conversely, a positive current was shown to degrade confinement. The symmetry found suggested searching magnitudes that may have changed sign under induction, *e.g.* the toroidal electric field and/or the global magnetic shear (as TJ-II vacuum rotational transform profiles are almost shearless). Hence, discrimination experiments to separate their roles were designed and performed [8].

These discrimination experiments consisted in comparing discharges with and without electron cyclotron current drive (ECCD) (*i.e.* changing the plasma current, I_p, while maintaining the toroidal electric field, E_t) that shared the same transformer action (which

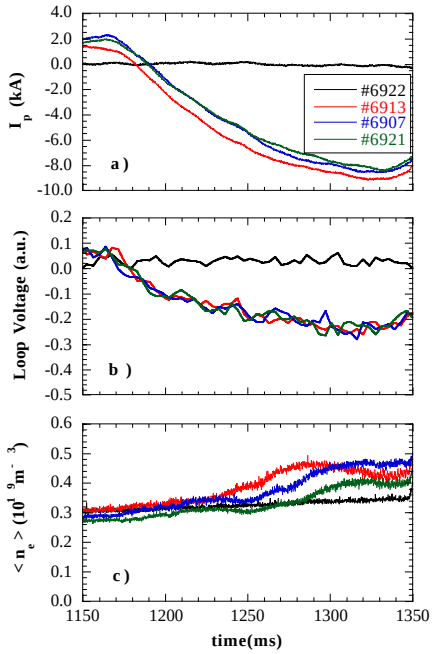

Fig. 2. Time evolution of net plasma current (a), loop voltage (b) and line-averaged density (c) in a set of four discharges: a reference one without induction (in black) and three discharges with equal transformer action but different ECCD: negative (#6913), null (#6917) and positive (#6921).

affects both I_p and E_t): *i.e.* if the plasma responds to E_t, then no delay between the start of ohmic induction and plasma response should be found among discharges with different ECCD levels and conversely. Moreover, in order to make temporal discriminations with low ECCD levels the discharges to be compared must have similar density values and need reference discharges without current drive. The experiments showed that significant changes in plasma densities are related to the inducted I_p, but not to E_t (Fig. 2). Studying the relation between density and I_p we found that, in the range of induced I_p, the average density $\tilde{n}_e$ behaves as follows: for positive $I_p \leq 5$ kA the $\tilde{n}_e$ decreases; for negative $I_p \leq 5$ kA, the $\tilde{n}_e$ increases, and for $|Ip| \geq 5$ kA, the $\tilde{n}_e$ increases.

A clear advantage of ohmic currents is that their profile can be reasonably inferred. Assuming that the actual knob for these observations is the global magnetic shear via plasma currents, then not only its magnitude, but also its sign, plays a role in confinement. Three complementary possibilities are suggested: i) MHD stability. Helical MHD modes can exist in TJ-II; their stability is dependent on the magnetic field rotational transform and shear. ii) Modification of particle orbits. This may affect considerably the fraction of direct particle losses in TJ-II. These losses can affect very differently the populations of passing and trapped particles depending on the rotational transform of the configuration. iii) Turbulent driven transport. Instabilities such as trapped electron modes depend both on local and global magnetic shear.

Electron internal transport barriers and role of rationals

Electron transport barriers have been observed in ECRH plasmas in stellarator devices, in plasmas regimes with high heating power density. These transitions are characterized by centrally peaked electron temperature profiles together with an improvement in core electron heat confinement. The influence of the magnetic topology on e-ITB formation has recently been experimentally studied in the TJ-II stellarator. A configuration scan (where iota was changed from 1.55 to 1.61) has shown that the plasma current value at which this transition takes place depends on the magnetic configuration: *i.e.* the higher the iota the higher the plasma current. This result points to the presence of a low order rational surface (n=3 / m=2) close to the plasma core as being a necessary condition for triggering e-ITB formation [9,10]. Kinetic effects induced by ECRH play also an important role for e-ITB triggering in this low collision regime.

HIBP measurements have permitted characterization of the plasma potential profile during e-ITB formation. The plasma potential increases in the plasma core region. Simultaneous measurements of the total beam intensity (proportional to plasma density) indicate that, at the transition, plasma density profiles are more hollow (Fig. 3). As a consequence, the radial

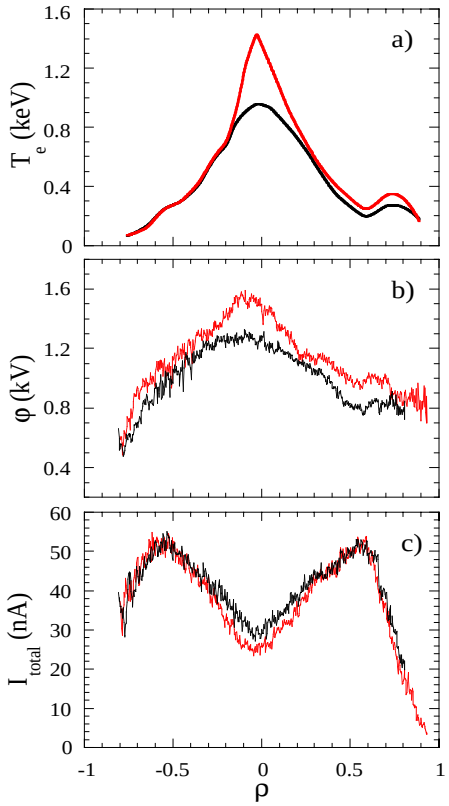

Fig. 3. Plasma profiles before (black) and during (red) the e-ITB: (a) electron temperature, (b) plasma potential and (c) beam intensity.

electric field increases from about 5 kV/m before to 15 kV/m during the e-ITB.

A transient behaviour with a rapid reduction in the core electron temperature, interpreted as the annihilation and creation of e-ITBs, was found in TJ-II plasmas with a rational surface close to the plasma core. The transient behaviour in plasma potential takes place in a time-scale of about 50 μs, which is much shorter than the energy confinement time, and it is dynamically coupled with perturbations in the core electron temperature and plasma density.

Biasing induced improved confinement regimes

Experimental results have shown that it is possible to modify global and edge plasma parameters with both positive and negative biasing (that is, an inner limiter biased positive or negative with respect to an outer limiter). Figure 4 shows the temporal evolution of plasma density, H_α monitors and edge ExB turbulent transport under negative biasing. The ratio between plasma density (n_e) and particle recycling, as quantified by H_α monitors, increases by up to a factor of two during negative limiter biasing together with a significant reduction in the turbulence level. A bursty-type behaviour in the H_α monitors, and evidence of MHD instabilities, has been observed during improved confinement regimes. Experimental results show the clear impact of these edge instabilities on (particle) confinement. The degree of modification of plasma confinement depends on different parameters: biasing voltage, plasma density as well as the radial location and the driven current of the biased limiters [11].

Edge as well as core plasma potentials are modified on two different time scales. In the rapid time scale (10 – 100 μs), the plasma potential changes in both the edge and core regions; in the slow time scale (1 – 10 ms) plasma potential modifications are linked to the evolution in the plasma density. The experimental results obtained can shed some light on quantifying the importance of neoclassical mechanisms when compared with anomalous ones in the study of the damping of the radial electric fields and flows in fusion plasmas.

Measurements of density and electron temperature profiles obtained by Thomson scattering during the negative biasing phase show that the density profile broadens while the temperature profile remains similar. An edge radial electric field, of the order of 100 V/cm, was measured by means of the HIBP diagnostic during the negative limiter biasing phase. Although radial electric fields are mainly modified in the proximity of the biased limiter, the plasma potential is affected across the whole plasma.

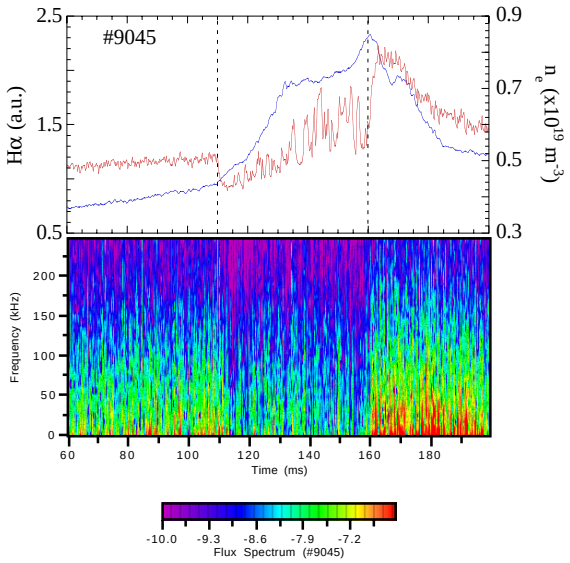

Fig. 4. Line average density and H_a signals and edge ExB turbulent transport during edge negative biasing.

It was also determined that, during limiter biasing, the spectral line intensities from inherent plasma impurities increase in proportion with the line-averaged electron density. Furthermore, the bolometer arrays, used to monitor the total radiation emitted along discharges, helped to show that the increase in total radiation observed during limiter biasing could be uniquely attributed to the increase in electron density, *i.e.* the electron temperature remained constant. The results and analysis of the data collected provide, by their consistency, significant evidence that limiter biasing in the TJ-II does not induce significant external influxes of impurities [12].

3. Transport studies

Impurity and particle transport studies

Transport studies on impurities injected into plasmas by the laser ablation method have been undertaken in various stellarators with the aim of obtaining localized information on transport coefficients in such devices. Previous experiments in TJ-II have shown that the decay of the perturbation created by the ablation can be analysed using a stretched exponential (of the type, $A_1\exp[-((t-t_0)/\tau)^{\beta}]$) and the impurity confinement times reach up to 100 ms [13].

Recently impurity transport has been investigated for a broad range of experimental situations in electron cyclotron heated plasmas (ECRH): *i.e.* for a density scan, a magnetic configuration scan, a power scan and its dependence with power deposition profile [14]. Figure 5 shows the dependence of impurity confinement for three different magnetic configurations ($\iota/2\pi$ =1.6, 1.8 and 2.2) and at several densities. The confinement time (τ) slowly increases with density up to a certain point where it increases more rapidly. Furthermore, this turning density is found to be higher for higher rotational transform values. Such behaviour resembles the spontaneous improvement in plasma bulk particle confinement at a critical density. The influence of ECRH power on impurity confinement time is shown in figure 6. Confinement time shows a strong dependence with ECRH heating power ($\tau \approx P^{-3}$) which turns out to be stronger than the one observed in the global energy confinement time ($P^{-0.5}$).

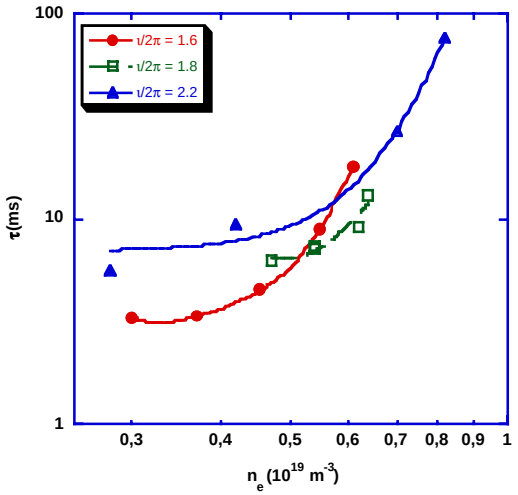

Fig. 5. Impurity (Si) confinement time versus plasma density at three different magnetic configurations.

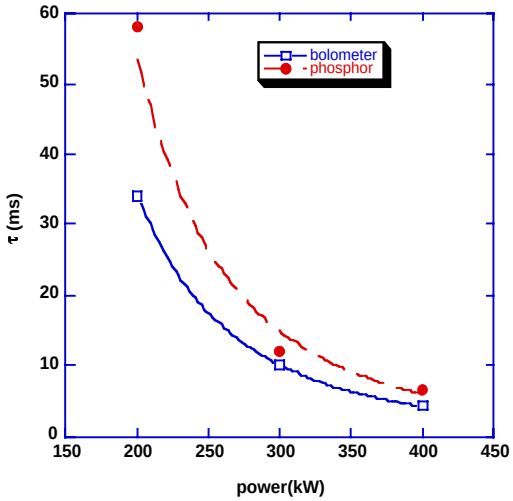

Fig. 6. Influence of ECRH heating on impurity (Si) confinement time.

It is useful to compare impurity and particle diffusivities in TJ-II. It is found that the impurity diffusion coefficient increases towards the plasma centre, where most of the injected power is deposited and that diffusion increases with power, most notably at the plasma core. The convective velocity is typically directed inward at radii less that r ≈ 0.5 and outward at larger radii. Similar behaviour was reported in W7-AS device [15]. Impurity diffusivities in the order 0.5 m^2/s ($\rho \approx 0.6$) and particle diffusivities in the range 0.2 m^2/s ($\rho \approx 0.6$) have been measured [13,16]. An inward pinch is necessary to explain the bulk particle transport.

However, evidence of non-diffusive transport mechanisms has been clearly observed during the propagation of edge cooling pulses experiments [17]. These studies have led to a reconsideration of diffusive transport, based on the Continuous Time Random Walk. A one-fluid toy model has been developed, incorporating a critical gradient mechanism that separates a sub-critical diffusive and a super-critical anomalous transport channel, depending on the local value of the gradient [18,19]. The model was found to produce stiff profiles, power degradation, an anomalous system size scaling of confinement, and rapid transport events, suggesting its general relevance to fusion transport studies. In the fluid limit, the model generates effective diffusive coefficients and pinch terms, which arise from the combination of finite-size particle steps and the critical mechanism, and may provide a partial explanation of the anomalous pinches observed in fusion experiments. Firm conclusions can however only be drawn on the basis of a more complete model (for at least two fields, n and T), which is currently under development.

Radial electric fields and transport

Radial plasma potential profiles have been obtained in the TJ-II by the HIBP diagnostic. These profiles show that the potential increases up to 1 kV near the magnetic axis in low-density plasmas ($n_e < 8 \times 10^{18}$ m^{-3}) (Fig. 7). In addition, the plasma potential shows a strong dependence on the plasma density. This finding is in reasonable agreement with neoclassical simulations for similar plasma conditions [20]. A recently developed Monte-Carlo code has been used to compute global ion fluxes in different TJ-II magnetic configurations [21]. These new simulations indicate that a non-local transport treatment might be important in complex devices like TJ-II. The secondary (Cs^{++}) beam ion current profiles, which directly reflect the plasma density, are hollow and in good agreement with Thomson scattering profiles. Such hollow profiles may be a manifestation of an outward particle flux induced by ECRH (*i.e.* the pump-out effect). As well, it has been experimentally observed that the modification of the profile shape is dependent on the position of low order rational surfaces, while the degree of profile hollowness is qualitatively correlated with the magnitude of the convective flux of ripple-trapped suprathermal electrons [22]. An approach based on Langevin equations has been recently developed to estimate this ECRH induced flux [23].

An ion power balance analysis based on central ion temperatures, obtained with a neutral particle analyser, and electron temperature and density profiles indicates the existence of two

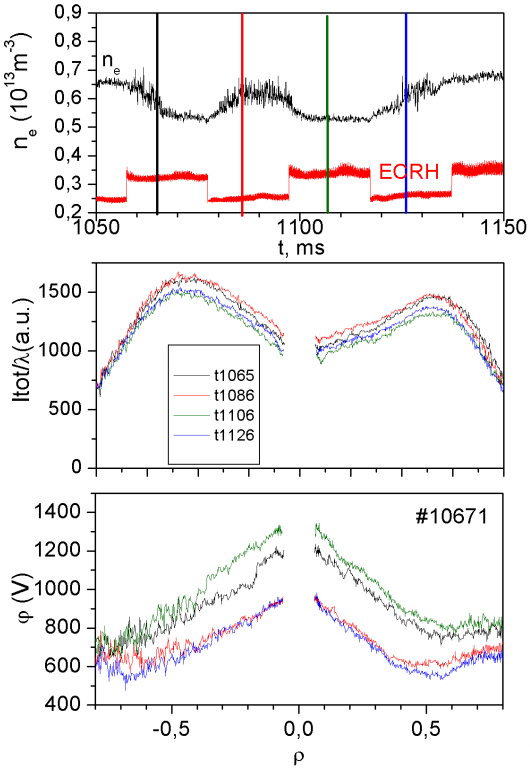

Fig.7. Time evolution of heating power and plasma density (top) and plasma potential and secondary Cs^{2+} ion profiles. Global plasma density decreases as ECRH power increases whereas plasma potential become more positive. Interestingly density profiles (as measured by the HIBP system) become more hollow.

different confinement regimes (which can be defined by electron-ion collisionality) characterized by two ion energy confinement times (both in the range of several ms) (Fig. 8). The transition between these regimes, which depends on wall conditioning, is also compatible with changes in the estimated ambipolar electric field deduced from neoclassical calculations [24].

The influence of low order rational surfaces (e.g. $n = 4/m = 2$ ($\iota(a)/2\pi \approx 2$) on the structure of parallel flows and plasma potential is under investigation. The presence of natural resonant surfaces has been deduced from a flattening observed in plasma-edge ion saturation current profiles, *i.e.* the floating potential becomes more positive and shows a significant radial variation. Quasi-coherent modes (of about 70 kHz), associated with the existence of rational surfaces, have been observed in the TJ-II. Moreover, differences in radial parallel-flow profiles exist in configurations with and without low-order rationals: a minimum appears to the outside of the rational location whereas this minimum does not appear in configurations free of rationals [25]. Also, radial plasma-potential profiles measured by the HIBP present evidence of structures in configurations with low order rational surfaces [26]. A possible explanation for such a flow structure near rational surfaces is the coupling of flow generation and turbulence [27]. This mechanism is consistent with the magnitude of the observed shearing rates (which are close to the critical value for reducing fluctuations) in the vicinity of a magnetic island. More recently it has been shown that, in the framework of neoclassical mechanisms, radial gradients can also be expected near rational surfaces in the radial electric fields [28].

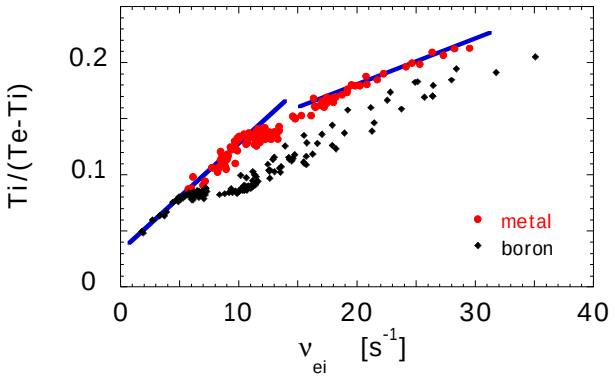

Fig. 8. Influence of plasma collisionality on ion transport.

4. Plasma – wall studies: divertor like configurations

Recent TJ-II experiments have been focussed in configurations with a low order rational value in the rotational transform located in the proximity of the last close flux surface (n = 4/m = 2) eventually leading to “local island divertor” topologies (Fig. 9). Hydrocarbon

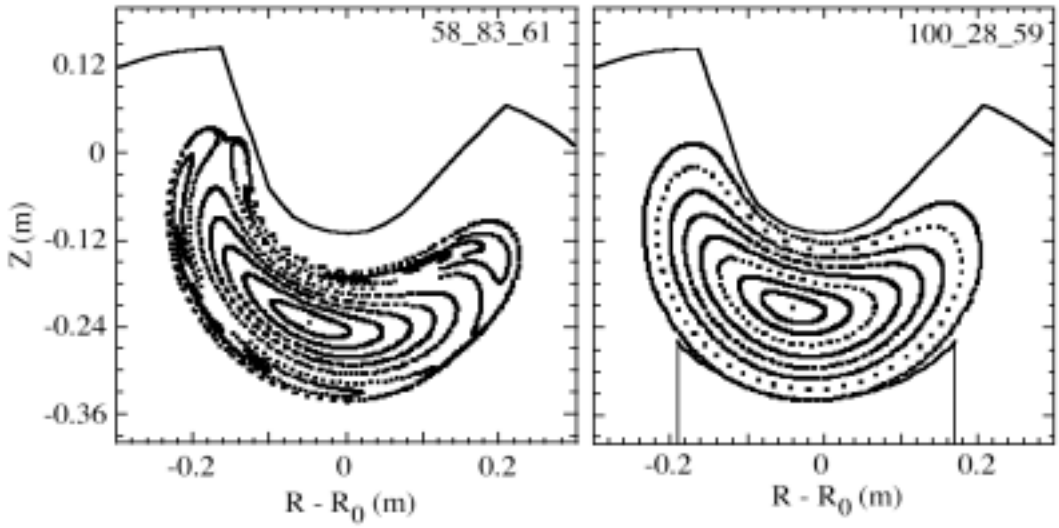

Fig. 9. Two examples of the magnetic configurations used in the experiments: an example of a "divertor-type" configuration (left): a "standard" configuration (right).

fuelling experiments in these configurations have been used to characterize the impurity screening properties related to the expected divertor effect (Fig. 10).

A significant different response to the same injected impurity was observed for edge-island configurations when compared to standard ones. Namely, a much lower increase of the normalized central carbon impurity (CV and CVI lines) takes place under "divertor" configuration scenarios. Also, the radial dependence of the fuelling efficiency is significantly different.

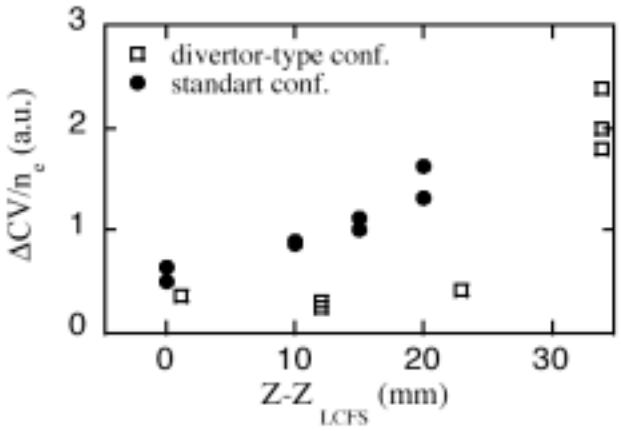

Fig. 10. Evolution of the normalized CV contamination at different radial positon of the impurity puff, for both configurations: Closed circles for "standard" and open squares for "divertor-type" configurations.

An almost flat, low efficiency is observed during the limiter insertion experiments until a critical position within the confined region is achieved. This position is well correlated with the nominal position of the actual separatrix. In standard configurations, however, a gradual increase of the fuelling efficiency is observed. Even when the starting point of these experiments corresponds to the confined region, the contamination of the plasma and its radial dependence with the source location suggest the presence of a weakly confining region in the last 2-3 cm of the plasma. The intrinsic contamination of the divertor-type configurations is systematically lower than that of conventional ones [29].

5. NBI plasmas

The first experiments with Neutral Beam Injection (NBI) heated plasmas have been performed. Flattened core electron temperatures in the range 200 to 300 eV and bell-shaped density profiles with $n_0 \leq 5x10^{19}$ m^{-3} are achieved in NBI plasmas (200 kW) (Fig. 11). In

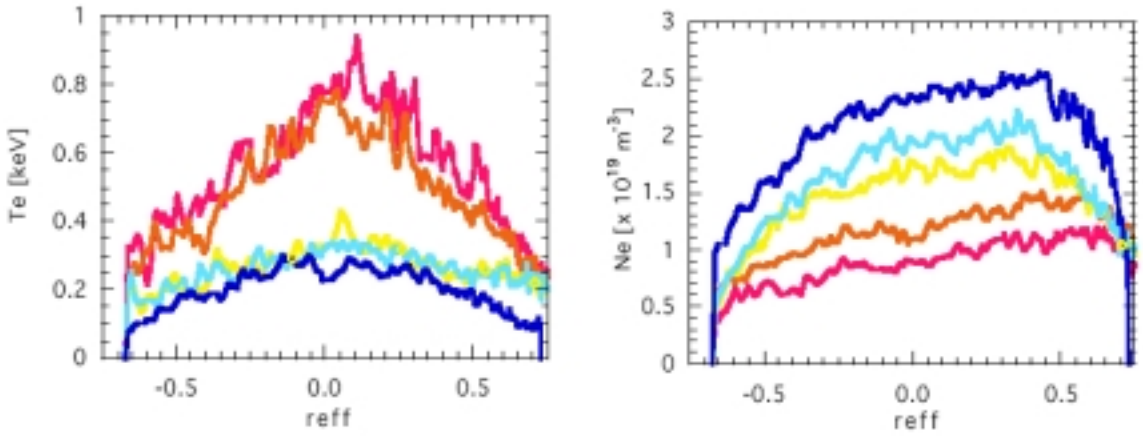

Fig. 11. Density and electron temperature profiles during the transition from ERCH (red) to NBI (blue) plasmas.

comparison, TJ-II ECRH (200–400 kW) plasmas show hollow density profiles with steep temperature profiles. Power balance estimates show that the NBI Thomson scattering profiles correspond to significant central power deposition.

The behaviour of the plasma ions and impurities has also been studied at the transition between ECH and NBI regimes. The ion temperature as measured by a Neutral Particle Analyzer shows non-Maxwellian spectra with a first slope that evolves from 90 eV under ECH to around 130 eV under NBI. Impurity temperature and rotation are monitored using passive emission spectroscopy. Toroidal rotation in both directions (co and counter) has been observed and it is seen to vary widely in magnitude (from a few to tens of km/s) [30].

Computer simulations of the beam-plasma interaction with the Monte-Carlo code FAFNER combined with the transport code PROCTR allow us to calculate NBI absorption, fuelling, and plasma electric field. The selfconsistent ambipolar radial electric field resulting from PROCTR is always negative with NBI, while for ECRH discharges it is positive near the axis. Preliminary measurements of plasma potential with the Heavy Ion beam diagnostic confirm the evolution of the electric field from positive at ECH plasmas to near sign reversal at the NBI regime.

Combined ECRH and NBI experiments reveal that, once ECRH heating power is switched-off, a confinement regime characterized by a strong reduction in ExB turbulence and a significant increase in the ratio between density (n) and particle recycling (H_α) is achieved. Several modes below 300 kHz have been found in the frequency spectra of magnetic pick-up coils in the NBI regime, which can be interpreted as Alfven modes. The SOL density decay length decreases to half its ECRH value and the tails in density profiles, currently observed in the SOL region in ECRH plasmas, disappear in the NBI phase. These results provide the first observation of direct link between the statistical properties of turbulent transport and non-exponential (and even flat) density profiles in the SOL region.

The maximum density reached ($4x10^{19}$ m^{-3}) falls within the stellarator density limit scaling law, suggesting that TJ-II NBI discharges terminate when its intrinsic density limit is reached. Experimental results suggest the importance of both radiative and edge transport mechanisms in the physics of the density limit of TJ-II.

Different combinations of gas puffing, ECH heating and wall conditioning strategies have been investigated with the aim of optimizing the power coupling and density control at NBI plasmas. Density control in NBI discharges with a plasma target created by on-axis ECH has proven difficult. Repeated wall cleaning seems to help only to the extent of smoothing the

density rise, although there appears no sign of stabilizing its value. On the contrary, target plasmas created by off-axis ECH, maintained during the NBI phase, are promising. In this way NBI plasma discharges with density control (up to 130 ms) have been obtained.

6. Conclusions

Significant improvements in characterising the confinement and stability properties of TJ-II stellarator plasmas have been achieved recently. The main conclusions can be summarized as follows:

1) Global confinement studies have shown a positive dependence of energy confinement on rotational transform and density.

2) Spontaneous and biasing-induced improved confinement transitions have been observed. The phenomelogy of TJ-II improved confinement regimes (a device designed for high beta operation but not optimized for neoclassical transport) looks similar to the H-mode regimes previously reported in stellarators. This similarity calls into question the leading role of neoclassical viscosity to access improved confinement regimes in stellarator devices.

3) Magnetic configuration scan experiments have highlighted the interplay between magnetic topology, transport and electric fields. The results obtained in TJ-II show that low-order rational surfaces modify radial electric fields, flows and transport. DC radial electric fields are comparable with those expected from neoclassical calculations. Magnetic shears affect transport. However, additional mechanisms based on neoclassical/turbulent E_r bifurcations and kinetic effects are needed to explain the impact of magnetic topology on transport.

4) Local transport studies have shown a dependence of plasma diffusivities and convective velocities on plasma density and heating power in consistence with global confinement properties.

5) Hydrocarbon fuelling experiments in configurations with a low order rational value in the rotational transform located in the proximity of the last close flux surface (n = 4/m = 2) have shown the impurity screening properties related to the expected divertor effect.

6) First experiments in NBI plasmas have been performed. The evolution of transport, density and turbulence at the transition from ECRH to NBI plasmas sustained plasmas points in the direction of an improved particle confinement regime.

[1] ASCASIBAR E. et al., “Confinement and stability on the TJ-II stellarator” Plasma Phys. and Cont. Fusion **44** (2002) B307
[2] CAPPA A. et al., “Electron energy distribution function during second harmonic ECRH plasma breakdown” Nuclear Fusion **44** (2004) 406.
[3] LINIERS M. et al., Fusion Technology **1** (1998) 307.
[4] TABARÉS F. et al. “Impact of wall conditioning and gas fuelling on the enhanced confinement modes in TJ-II” J. Nuclear Materials **313** (2003) 839
[5] GARCÍA - CORTÉS I. et al. “Spontaneous improvement of TJ-II plasmas confinement” Plasma Phys. Control. Fusion **44** (2002) 1639.
[6] HIDALGO C. et al., “Experimental evidence of coupling between sheared flows development and an increasing in the level of turbulence in the TJ-II stellarator” Physical Review E (in press)

[7] ROMERO J. et al., "Controlling confinement with induced toroidal current in the flexible Heliac TJ-II" Nuclear Fusion **43** (2003) 386.
[8] LÓPEZ BRUNA D. et al., "Effects of Ohmic current in the TJ-II stellarator" Nuclear Fusion **44** (2004) 645
[9] ESTRADA T., et al., "Electron internal transport barrier formation and dynamics in the plasma core of the TJ-II stellarator" Plasma Phys. Contr. Fusion **46** (2004) 277-286
[10] CASTEJÓN F. et al," Influence of low-order rational magnetic surfaces on heat transport in TJ-II heliac ECRH plasmas" Nuclear Fusion **42** (2004).
[11] HIDALGO C. et al., "Improved confinement regimes induced by limiter biasing in the TJ-II stellarator" Plasma Phys. and Control. Fusion **45** (2004) 287.
[12] McCARTHY K. J. et al., "A first study of impurity behaviour during externally induced radial electrical fields in the TJ-II stellarator" Fusion Technology **46** (2004) 129
[13] ZURRO B. et al., "Transport analysis of impurity injected by laser ablation in the TJ-II stellarator" Proc. 30 th EPS (2003).
[14] ZURRO B. et al., "Impurity transport and confinement in the TJ-II Stellarator" Proc. IAEA Fusion Energy Conference Vilamoura (2004).
[15] BURHENN R. et al., "Derivation of local impurity transport quantities from soft-x radiation evolution during tracer injection at W7-AS" Rev. Sci. Instrum. **70** (1999) 603.
[16] EGUILIOR S. et al., "Perturbative particle transport experiments on TJ-II stellarator" Proc 14th International Stellarator Workshop (2003).
[17] VAN MILLIGEN B. et al., "Ballistic transport phenomena in TJ-II" Nuclear Fusion **42** (2002) 787.
[18] VAN MILLIGEN B. et al., "Uphill transport and the probabilistic transport model " Plasma physics **11** (2004) 3787.
[19] VAN MILLIGEN B. et al., "Probabilistic finite-size transport models for fusion: Anomalous transport and scaling laws" Phys. Plasmas **11** (2004) 2272
[20] TRIBALDOS V., "Monte Carlo estimation of neoclassical transport for the TJ-II stellarator" Phys. Plasmas **8** (2001) 1229
[21] TRIBALDOS V. et al., Plasma Physics and Control. Fusion (2004) (submitted).
[22] OCHANDO M. A. et al., "Emissivity toroidal asymmetries induced by ECRH driven convective fluxes in the TJ-II stellarator" Plasma Phys. Control. Fusion 45, 221 (2003).
[23] CASTEJÓN F. et al.Plasma Physics and Cont. Fusion **45** (2003) 159
[24] BALBÍN R. et al., "Ion confinement studies on the TJ-II stellarator" Proc 14th International Stellarator Workshop (2003)
[25] PEDROSA M.A. et al., "Interplay between parallel and perpendicular sheared flows and fluctuations in the plasma boundary region of the TJ-II stellarator" Plasma Phys. Control. Fusion **46** (2004) 221.
[26] KRUPNIK L. et al., "Radial electric fields and confinement in the TJ-II stellarator" Proc. 31th EPS Conf. (2004).
[27] HIDALGO C. et al., "Fluctuations, sheared radial electric fields and transport interplay in fusion plasmas" New Journal of Physics **5** (2002) 51.
[28] SHAING K. C. et al., "Plasma and momentum transport processes in the vicinity of a magnetic island in a tokamak" Nucl. Fusion **43** (2003) 258.
[29] GARCÍA-CORTÉS I. et al., "Fuelling efficiency of Hydrocarbons in TJ-II plasmas" J. Nucl. Materials (2004) (in press)
[30] RAPISARDA D. et al., "Toroidal rotation of protons and impurities in the TJ-II stellarator: ECRH versus umbalanced NBI" Proc. 31th EPS Conf. (2004).